REVIEW

DILL EXTRACT AS GREEN INHIBITOR FOR THE CORROSION OF CARBON STEEL IN H_3PO_4 SOLUTION

KAMAL SHALABI[1], ABDELAZIZ S. FOUDA[1], AYMAN Y. EL-KHATEEB[2], NEHAL M. SALEM[1]

Manuscript received: 12.01.2013; Accepted paper: 20.02.2013;

Published online: 01.03.2013.

Abstract. *The inhibiting effect of dill extract (DE) on the corrosion of C-steel in 1 N H_3PO_4 was studied by weight loss, potentiodynamic polarization, electrochemical impedance spectroscopy (EIS). The results showed that the inhibition efficiency increases with increasing the inhibitor concentration, while it decreases with increasing the temperature. The adsorption of dill extract on the C-steel surface obeys Langmuir adsorption isotherm. Some thermodynamic parameters were calculated and discussed. The values of free energy of adsorption for investigated inhibitors were calculated. Polarization curves show that dill extract is mixed-type inhibitors. The results obtained from chemical and electrochemical techniques are in good agreement.*

Keywords: *C-steel, Potentiodynamic polarization, EIS, Dill, acid corrosion.*

1. INTRODUCTION

Corrosion is a fundamental process playing an important role in economics and safety, particularly for metals. The use of inhibitors is one of the most practical methods for protection against corrosion, especially in acidic media [1]. Most well-known acid inhibitor are organic compounds containing nitrogen , sulfur, and oxygen atoms. Among them, organic inhibitors have many advantages such as high inhibition efficiency, low price, low toxicity, and easy production [2-5]**.**Organic heterocyclic compounds have been used for the corrosion inhibition of iron [6-9], copper [10], aluminum [11-13], and other metals [14-15] in different corroding media. Although many of these compounds have high inhibition efficiencies, several have undesirable side effects, even in very small concentrations, due to their toxicity to humans, deleterious environmental effects, and high-cost [16].

Plant extract is low-cost and environmental safe, and so the main advantage of using plant extract as the corrosion inhibitor is due to both economic and environmental benefits. Up to now, many plant extracts have been used as effective corrosion inhibitors of iron or steel in acidic media, such as *Azadirachta* [17], *Vernonia amygdalina* [18], *Henna* [19], *Nypa fruticans Wurmb* [20], *Zenthoxylum alatum* [21], *Damsissa* [22], *Mentha pulegium* [23], olive [24], *Phyllanthus amarus* [25], *Occimum viridis* [26], lupine [27], *Lasianthera africana* [28], *Strychnos nux-vomica* [29], *Justicia gendarussa* [30], *Oxandra asbeckii* [31], *Ferula assafoetida* [32], coffee [33], fruit peel [34] and Halfabar [35]. The inhibition performance of plant extract is normally ascribed to the presence of complex organic species, including tannins, alkaloids and nitrogen bases, carbohydrates and proteins as well as hydrolysis

[1] Mansoura University, Faculty of Science, 35516 Mansoura, Egypt. E-mail: dr_kemo84@yahoo.com.
[2] Mansoura University, Faculty of Agriculture, 35516 Mansoura, Egypt.

products in their composition. These organic compounds usually contain polar functions with nitrogen, sulfur, or oxygen atoms as well as those with triple or conjugated double bonds or aromatic rings in their molecular structures, which are the major adsorption centers.

The objective of this study was to investigate the inhibitory effects of dill extract as a corrosion inhibitor for carbon steel in 1 N H_3PO_4 acid by using weight loss, potentiodynamic polarization, electrochemical impedance spectroscopy and electrochemical frequency modulation methods.

2. MATERIALS AND METHODS

2.1. MATERIALS

Tests were performed on C-steel specimens of the following composition (weight %):0.200 % C, 0.350 % Mn, 0.024 % P, 0.003 % S, and the remainder Fe.

2. 2. PREPARATION OF PLANT EXTRACTS

Fresh aerial parts of dill were collected from Mansura University fields, Mansoura, Egypt in August 2012. Then identified by Botany Department, Faculty of Science, Mansoura University. The sample was cut into small pieces, thoroughly washed with distilled water dried for a prolong period of time, grounded into powder and weighed (100 grams). Powdered material of the plant was extracted separately by soaking at room temperature for six times with methanol (5L), then the methanolic extracts of the samples were concentrated to nearly dryness under reduced pressure by using the rotatory evaporator at 45°C to achieve the crude methanolic extracts which kept for further investigation.

2.2.1. Phytochemistry of investigated plant

The main constituents of dill extract are a mixture of α-phellandrene, eugenol, anethole, flavonoids, coumarins, triterpenes, phenolic acids and umbelliferones [36].

Chemical structure of dill

Dillapiol

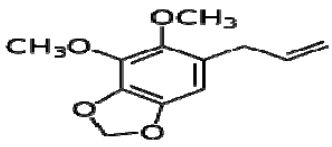

Limonene

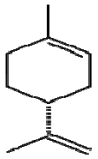

Carvone

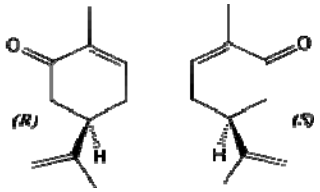

Myristicin

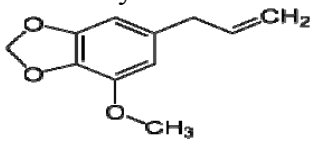

Eugenol

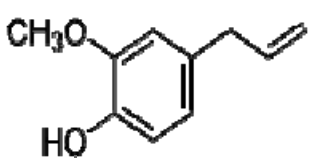

Terpinene

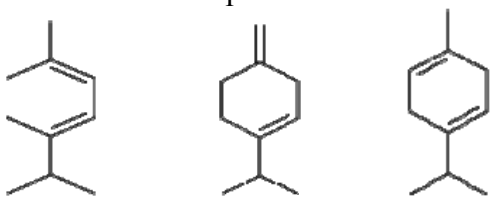

α-Terpinene β-Terpinene γ-Terpinene

2.3. SOLUTIONS

The aggressive solutions, 1N H_3PO_4 were prepared by dilution of analytical grade (85%) H_3PO_4 with bi-distilled water. The concentration range of the inhibitor used was (20-120 ppm).

2.4. WEIGHT LOSE MEASUREMENTS

Seven parallel C-steel sheets of 2.5 × 2.0 × 0.06 cm were abraded with emery paper (grade 320–500–800) and then washed with bidistilled water and acetone. After accurate weighing, the specimens were immersed in a 250 ml beaker, which contained 250 ml of HCl with and without addition of different concentrations of dill extract.

All the aggressive acid solutions were open to air. After 3 h, the specimens were taken out, washed, dried, and weighed accurately. The average weight loss of seven parallel C-steel sheets could be obtained. The inhibition efficiency (IE%) and the degree of surface coverage, θ, of dill extract for the corrosion of C-steel were calculated as follows [37],

$$IE\% = \theta \times 100 = \left[1 - \frac{W}{W^{o}}\right] \times 100 \quad (1)$$

where Wº and W are the values of the average weight loss without and with addition of the inhibitor, respectively.

2.5. ELECTROCHEMICAL MEASUREMENTS

Electrochemical experiments were performed using a typical three-compartment glass cell consisted of the C-steel specimen as working electrode (1 cm^2), saturated calomel electrode (SCE) as a reference electrode and a platinum foil (1.0 cm2) as a counter electrode. The reference electrode was connected to a Luggin capillary and the tip of the Luggin capillary is made very close to the surface of the working electrode to minimize IR drop. All the measurements were done in solutions open to atmosphere under unstirred conditions. All potential values were reported versus SCE. Prior to every experiment, the electrode was abraded with successive different grades of emery paper, degreased with acetone and washed with bidistilled water and finally dried.

Tafel polarization curves were obtained by changing the electrode potential automatically from (-1.3 to 0.5 V vs. SCE) at open circuit potential with a scan rate of 1 mVs-1. Stern-Geary method [38] used for the determination of corrosion current is performed by extrapolation of anodic and cathodic Tafel lines of charge transfer controlled corrosion reactions to a point which gives log i_{corr} and the corresponding corrosion potential (E_{corr}) for inhibitor free acid and for each concentration of inhibitor. Then i_{corr} was used for calculation of inhibition efficiency (IE %) and surface coverage (θ) as below:

$$IE\% = \theta \times 100 = \left[1 - \frac{i_{corr(inh)}}{i_{corr(free)}}\right] \times 100 \quad (2)$$

where $i_{corr(free)}$ and $i_{corr(inh)}$ are the corrosion current densities in the absence and presence of inhibitor, respectively.

Impedance measurements were carried out in frequency range from 100 kHz to 0.1Hz with amplitude of 5 mV peak-to-peak using ac signals at open circuit potential. The experimental impedance was analyzed and interpreted based on the equivalent circuit. The main parameters deduced from the analysis of Nyquist diagram are the resistance of charge transfer R_{ct} (diameter of high-frequency loop) and the capacity of double layer C_{dl}. The inhibition efficiencies (IE %) and the surface coverage (θ) obtained from the impedance measurements are defined by the following relations:

$$IE\% = \theta \times 100 = \left[1 - \frac{R^{o}_{ct}}{R_{ct}}\right] \times 100 \quad (3)$$

where R^{o}_{ct} and R_{ct} are the charge transfer resistance in the absence and presence of inhibitor, respectively.

The electrode potential was allowed to stabilize 30 min before starting the measurements. All the experiments were conducted at 25 ± 1°C. Measurements were performed using Gamry Instrument Potentiostat / Galvanostat /ZRA. This includes a Gamry framework system based on the ESA 400. Gamry applications include DC105 for potentiodynamic polarization measurements and EIS300 for electrochemical impedance spectroscopy measurements along with a computer for collecting data. Echem Analyst 6.03 software was used for plotting, graphing, and fitting data.

To test the reliability and reproducibility of the measurements, duplicate experiments were performed in each case at the same conditions.

3. RESULTS AND DISCUSSION

3.1. WEIGHT LOSS MEASUREMENTS

The weight loss-time curves of C-steel with the addition of dill extract in 1N H_3PO_4 at various concentrations is shown in Fig. 1. The curve of Fig. 1 shows that the weight loss values of C-steel in 1N H_3PO_4 solution containing dill extract decrease as the concentration of the inhibitor increases; i.e., the corrosion inhibition strengthens with the inhibitor concentration, this is appear in the Table 1.This trend may result from the fact that the adsorption of inhibitor on the C-steel increases with the inhibitor concentration thus the C-steel surface is efficiently separated from the medium by the formation of a film on its surface [39].

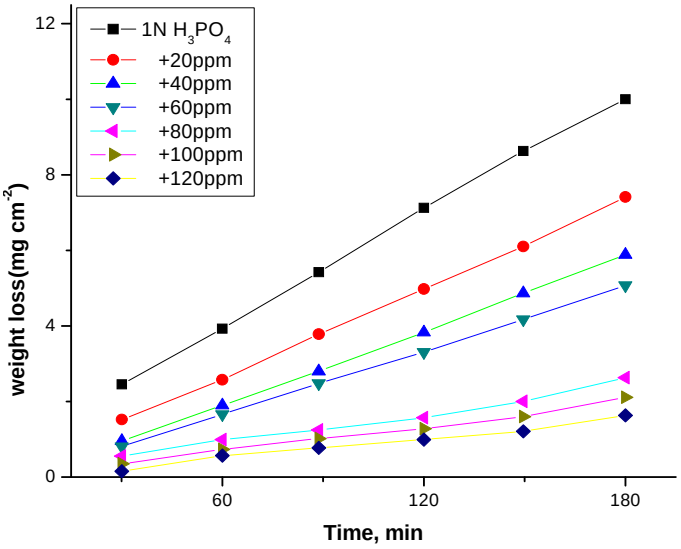

Fig. 1. Weight loss- time curves for the corrosion of C-steel in 1N H_3PO_4 in the absence and presence of different concentrations of dill extract at 30°C.

Table 1. Variation of inhibition efficiency (%IE) of different compounds with their molar concentrations at 30°C from weight loss measurements at 180 min immersion in 1N H_3PO_4.

Concentration [ppm]	Corrosion rate [mg cm^{-2} min^{-1}]	θ	IE%
1N H_3PO_4	0.0510		
20	0.0393	0.230	23.0
40	0.0330	0.354	35.4
60	0.0283	0.445	44.5
80	0.0131	0.743	74.3
100	0.0111	0.782	78.2
120	0.0091	0.822	82.2

3.2. POTENTIODYNAMIC POLARIZATION TECHNIQUE

Fig. 2 shows the anodic and cathodic Tafel polarization curves for C-steel in 1N H_3PO_4 in the absence and presence of varying concentrations of dill extract at 25 °C respectively. From Fig. 2, it is clear that both anodic metal dissolution and cathodic H_2 reduction reactions were inhibited when investigated inhibitors were added to 1N H_3PO_4 and this inhibition was more pronounced with increasing inhibitor concentration. Tafel lines are shifted to more negative and more positive potentials with respect to the blank curve by increasing the concentration of the investigated inhibitors.

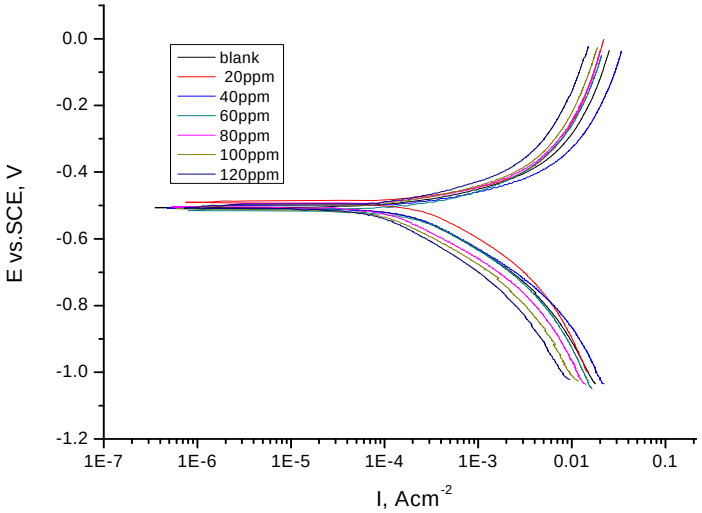

Fig. 2. Potentiodynamic polarization curves for corrosion of C-steel in 1N H_3PO_4 in the absence and presence of different concentrations of dill extract at 25 °C.
of dill extract at 30°C.

This behavior indicates that the undertaken additives act as mixed-type inhibitors [39-40]. The results in Table 2 show that the increase in inhibitor concentration leads to decrease the corrosion current density (i_{corr}), but the Tafel slopes (β_a , β_c),are approximately constant indicating that the retardation of the two reactions (cathodic hydrogen reduction and anodic metal dissolution) were affected without changing the dissolution mechanism[41-43].

Table 2. The effect of concentration of the investigated compounds on the free corrosion potential (E_{corr}), corrosion current density (i_{corr}), Tafel slopes (βa& βc), inhibition efficiency (% IE) ,degree of surface coverage (θ) and corrosion rate(CR) for the corrosion of C-steel in 1N H_3PO_4 at 25°C.

Concentration ppm	i_{corr} uA	E_{corr} mV	βa mV/decade	βc mV/decade	CR mpy	ϴ	%IE
blank	555.0	-507	250.9	245.8	91.36		
20	200.0	-490	195.4	202.6	91.36	0.64	63.96
40	130.0	-507	196.7	173.8	59.59	0.77	76.58
60	54.5	-514	180.2	185.7	24.92	0.90	90.18
80	43.1	-504	179.0	101.8	19.71	0.92	92.23
100	40.5	-508	181.0	129.2	18.52	0.93	92.70
120	14.2	-505	157.8	124.4	6.467	0.97	97.00

3.3. ELECTROCHEMICAL IMPEDANCE SPECTROSCOPY (EIS)

The effect of inhibitor concentration on the impedance behavior of C-steel in 1N H_3PO_4 solution at 25 ºC is presented in Fig. 3 (a, b). The curves show a similar type of Nyquist plots (Fig.3a) for C-steel in the presence of various concentrations of dill extract. The existence of single semi-circle showed the single charge transfer process during dissolution which is unaffected by the presence of inhibitor molecules. Deviations from perfect circular shape are often referred to the frequency dispersion of interfacial impedance, which arises due to surface roughness, impurities, dislocations, grain boundaries, adsorption of inhibitors, and formation of porous layers and in homogenates of the electrode surface [44-45]. Inspections of the data reveal that each impedance diagram consists of a large capacitive loop with one capacitive time constant in the Bode–phase plots (Fig.3b). The electrical equivalent circuit model is shown in Fig. 4. It used to analyze the obtained impedance data. The model consists of the solution resistance (R_s), the charge-transfer resistance of the interfacial corrosion reaction (R_{ct}) and the Constant phase element (CPE). Excellent fit with this model was obtained with our experimental data. The values of the interfacial capacitance C_{dl} can be calculated from CPE parameter values Y_0 and n using the expression [46]:

$$C_{dl} = Y_{0(\omega_{\max})^{n-1}} \tag{4}$$

where Y_0 is the magnitude of the CPE, ω is the angular frequency at which the imaginary component of the impedance reaches its maximum values and n is the deviation parameter of the CPE: $-1 \leq n \leq 1$. EIS data (Table 3) show that the R_{ct} values increases and the C_{dl} values decreases with increasing the inhibitor concentrations. This is due to the gradual replacement of water molecules by the adsorption of the inhibitor molecules on the metal surface, decreasing the extent of dissolution reaction. The higher (R_{ct}) values, are generally associated with slower corroding system [47-48].

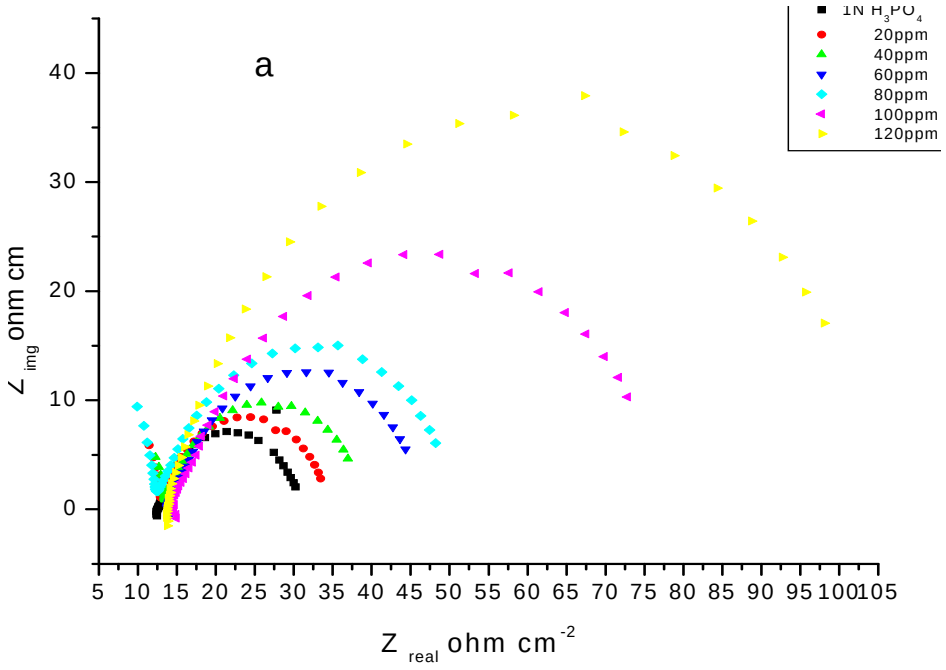

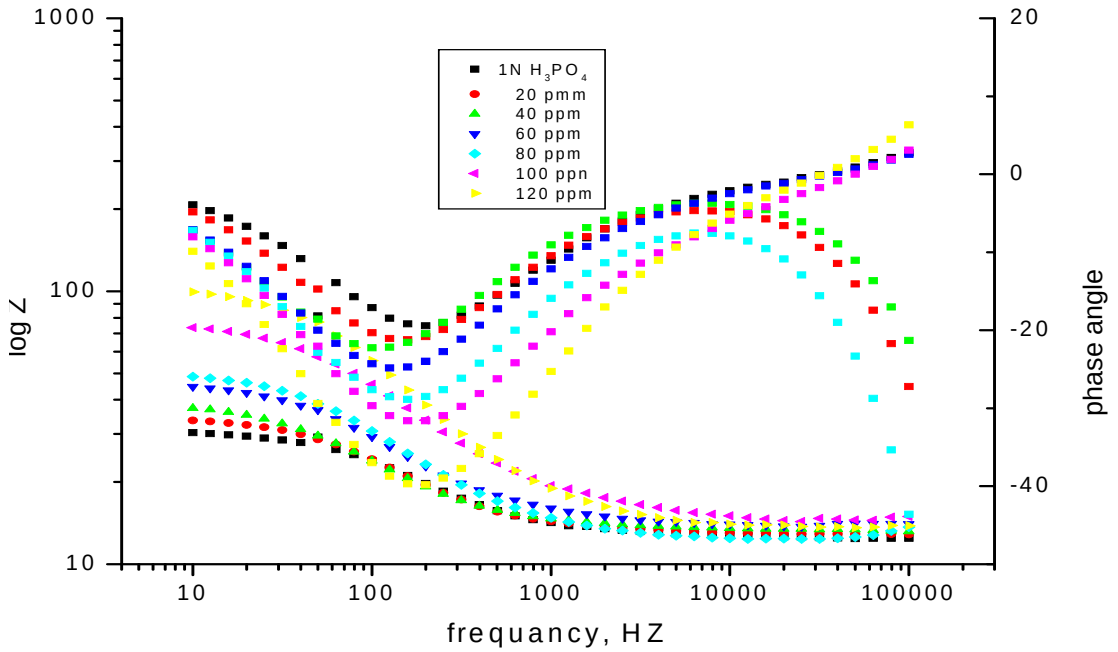

Fig. 3. The Nyquist (a) and Bode (b) plots for corrosion of C-steel in 2M HCl in the absence and presence of different concentrations of compound (1) at 25°C.

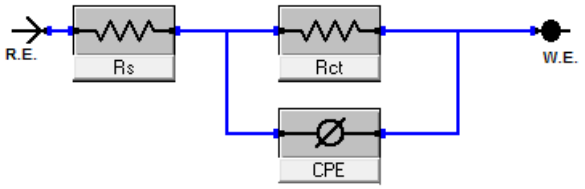

Fig. 4. Electrical equivalent circuit model used to fit the results of impedance.

Table 3. EIS data of C-steel in 1N H_3PO_4 and in the absence and presence of different concentrations of investigated inhibitors at 25 °C.

Concentration [ppm]	R_{ct}, [ohm cm^2]	C_{dl} [F $x10^{-5}$]	Θ	%IE
1N H_3PO_4	18.87	9.47		
20	24.05	8.58	0.215	21.5
40	27.91	8.07	0.324	32.4
60	33.90	7.02	0.443	44.3
80	46.23	6.65	0.592	59.2
100	66.06	3.67	0.714	71.4
120	94.29	2.91	0.800	80.0

The decrease in the C_{dl} can result from the decrease of the local dielectric constant and/or from the increase of thickness of the electrical double layer suggested that the inhibitor molecules function by adsorption at the metal/solution interface [49]. The IE% obtained from EIS measurements are close to those deduced from weight loss and polarization measurements.

3.4. ADSORPTION ISOTHERM

It is generally assumed that the adsorption of the inhibitors on the metal surface is the essential step in the inhibition mechanism [50]. To calculate the surface coverage θ it was assumed that the inhibitor efficiency is due mainly to the blocking effect of the adsorbed

species and hence *IE %= 100 x θ* [51]. In order to gain insight into the mode of adsorption of the extract on C-steel surface, the surface coverage values from weight loss technique were theoretically fitted into different adsorption isotherms and the values of correlation coefficient (R^2) were used to determine the best-fit isotherm. Fig. 5 shows the plot $\theta/(1-\theta)$ vs. C which is typical of Langmuir adsorption isotherm. Perfectly linear plot was obtained with regression constant (R^2) exceeded 0.97 and slope about unity. The Langmuir isotherm is given as [52]:

$$\frac{\theta}{(1-\theta)} = K_a C \tag{5}$$

where C is the inhibitor concentration and K_a is the equilibrium constant of adsorption process and is related to the standard free energy of adsorption ΔG°_{ads} by the equation:

$$K_a = \frac{1}{5.55} e^{\frac{-\Delta G^{o}_{ads}}{RT}} \tag{6}$$

The value of 5.55 is the concentration of water in solution expressed in mole per liter, R is the universal gas constant and T is the absolute temperature.

The deviation of the slope from unity as observed from this study could be interpreted to mean that there are interaction between adsorbate species on the metal surface as well as changes in adsorption heat with increasing surface coverage [53, 54], factors that were ignored in the derivation of Langmuir isotherm.

The calculated ΔG°_{ads} values were also given in Table 4. The negative values of ΔG°_{ads} ensure the spontaneity of the adsorption process and the stability of the adsorbed layer on the C-Steel surface. It is well known that values of ΔG°_{ads} of the order of -40 kJ mol^{-1} or higher involve charge sharing or transfer from the inhibitor molecules to metal surface to form coordinate type of bond (chemisorption); those of order of -20 kJ mol^{-1} or lower indicate a physisorption [55-56]. The calculated ΔG°_{ads} values (Table 4) are less negative than -20 $kJmol^{-1}$ indicate, therefore, that the adsorption mechanism of the investigated extract on C-steel in 1N H_3PO_4 solution is typical of physisorption. The lower negative values of ΔG°_{ads} indicate that this inhibitor is not strongly adsorbed on the C-Steel surface.

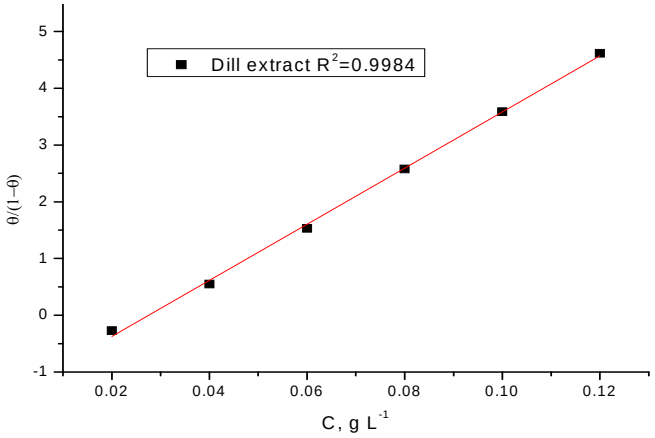

Fig. 5. Curve fitting of corrosion data for C-steel in 1N H_3PO_4 in the presence of different concentrations of dill extract to Langmuir adsorption isotherm at 30 °C.

Table 4. Equilibrium constant (K_{ads}) and adsorption free energy (ΔG°_{ads}) of STE adsorbed on C-steel surface in 1N H_3PO_4 at 25 °C.

Langmuir adsorption isotherm		
ΔG°_{ads} [kJ mol^{-1}]	K_{ads} x 10^{-5} [L g^{-1}]	
-19.62	49.45	DE

3.5. EFFECT OF TEMPERATURE

The effect of temperature on the rate of corrosion of C-steel in 1N H_3PO_4 containing different concentration from dill extract was tested by weight loss measurements over a temperature range from 30 to 60 ^oC.

The results revealed that, the rate of corrosion increases as the temperature increases and decreases as the concentration of these compounds increases for all compound used. The activation energy (E^*_a) of the corrosion process was calculated using Arrhenius equation:

$$k = Ae^{\frac{-E_a^*}{RT}} \quad (7)$$

where k is the rate of corrosion, A is the Arrhenius constant, R is the gas constant and T is the absolute temperature.

Fig. 6 presents the Arrhenius plot in the presence and absence of dill extract. E^*_a values determined from the slopes of these linear plots are shown in Table 5. The linear regression (R^2) is close to 1 which indicates that the corrosion of C-steel in 1N H_3PO_4 solution can be elucidated using the kinetic model. Table 4 showed that the value of E^*_a for inhibited solution is higher than that for uninhibited solution, suggesting that dissolution of C-steel is slow in the presence of inhibitor and can be interpreted as due to physical adsorption [57]. It is known from Eq. 7 that the higher E^*_a values lead to the lower corrosion rate. This is due to the formation of a film on the C-steel surface serving as an energy barrier for the C-steel corrosion [58].

Enthalpy and entropy of activation (ΔH^*, ΔS^*) of the corrosion process were calculated from the transition state theory (Table 5):

$$k = \left(\frac{RT}{Nh}\right) e^{\frac{\Delta S^*}{R}} e^{\frac{-\Delta H^*}{RT}} \quad (8)$$

where h is Planck's constant and N is Avogadro's number.

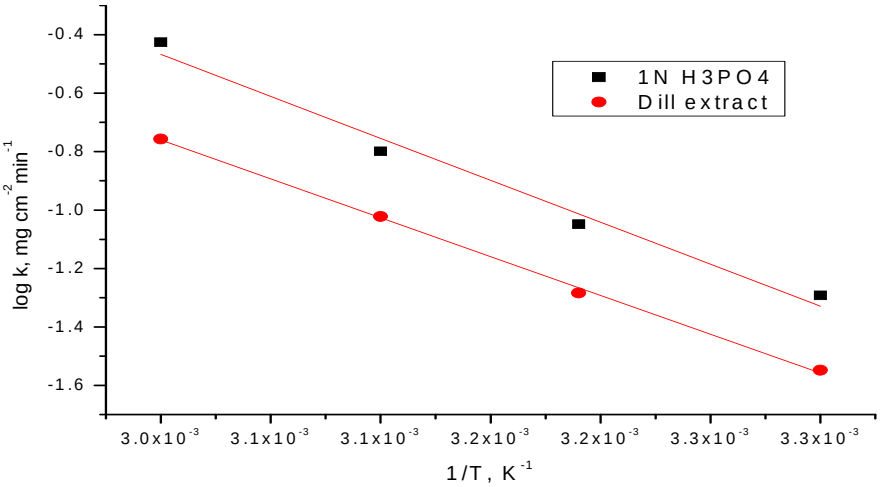

Fig. 6. log k – 1/T curves for C-steel dissolution in 1N H_3PO_4 in the absence and presence of 120 ppm of dill extract.

A plot of log (Rate/ T) vs. 1/ T for C-steel in 1N H_3PO_4 at different concentrations from dill extract, gives straight lines as shown in Fig. 7 for dill extract. The positive signs of ΔH^* reflect the endothermic nature of the steel dissolution process. Large and negative values of ΔS^* imply that the activated complex in the rate-determining step represents an association rather than dissociation step, meaning that decrease in disordering takes place on going from reactants to the activated complex [59-60].

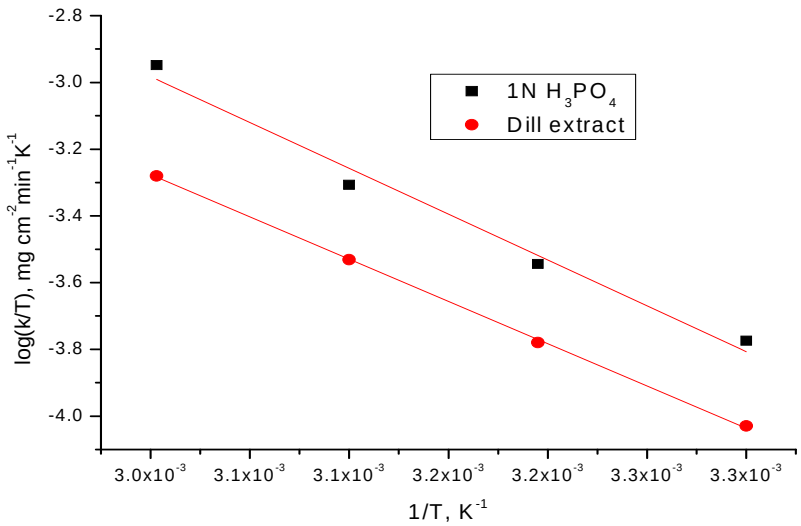

Fig. 7. log k/T – 1/T curves for C-steel dissolution in 1N H_3PO_4 in the absence and presence of 120 ppm of dill extract.

Table 5 Activation parameters of the corrosion of C-steel in 1N H_3PO_4 at 120 ppm for dill extract.

Inhibitor	ΔE_a*, [kJ mol^{-1}]	ΔH*, [kJ mol^{-1}]	ΔS*, [J $mol^{-1}K^{-1}$]
1N H_3PO_4	47.06	40.93	-141.8
Dill extract	54.67	50.61	-112.0

3.6. MECHANISM OF THE INHIBITION

Most organic inhibitors contain at least one polar group with an atom of nitrogen or sulphur or in some cases selenium and phosphorus. The inhibiting properties of many compounds are determined by the electron density at the reaction center [61]. With increase in electron density in the center, the chemisorption between the inhibitor and the metal are strengthened [62, 63]. The plant extract DE contains the phytochemical constituents such as α-phellandrene, eugenol, anethole, flavonoids, coumarins, triterpenes, phenolic acids and umbelliferones. There are two modes of adsorption considered on the metal surface in acid media. In the first one, the neutral molecules may be adsorbed on the surface of carbon steel through the chemisorptions mechanism, involving the displacement of water molecules from the carbon steel surface and the sharing electrons between the hetero-atoms and iron. The inhibitor molecules can also adsorb on the carbon steel surface on the basis of donor – acceptor interactions between π-electrons of the aromatic ring and vacant d-orbitals of surface iron atoms. In the second mode, since it is well known that the steel surface bears positive charge in acid solution [64, 65], so it is difficult for the protonated molecules to approach the positively charged carbon steel surface due to the electrostatic repulsion. Since Phospate ions have a smaller degree of hydration, thus they could bring excess negative charges in the vicinity of the interface and favor more adsorption of the positively charged inhibitor molecules, the above said phytochemical constituents present in DE, having many active centers such as nitrogen, sulphur and oxygen, are adsorbed through electrostatic interactions between the positively charged molecules and the negatively charged metal surface. Thus there is a synergism between adsorbed PO_4^{3-}ions and active centers presented in DE. Thus we can conclude that inhibition of carbon steel corrosion in 1N H_3PO_4 is mainly due to electrostatic interaction. The decrease in the inhibition efficiency with rise in temperature

supports electrostatic interaction. In the current investigation the DE was found to perform as a good inhibitor for C-steel corrosion.

4. CONCLUSIONS

The dill extract establish a very good inhibition for C-steel corrosion in H_3PO_4 solution.

Dill extract inhibit C-steel corrosion by adsorption on its surface and act better than the passive oxide film.

The inhibition efficiencies of the dill extract increase with increasing of its concentrations and decrease with increasing of the temperature.

Double layer capacitances decrease with respect to blank solution when the inhibitor added. This fact may explained by adsorption of the inhibitor molecule on the C-steel surface.

The adsorption of these compounds on C-steel surface in H_3PO_4 solution follows Langmuir adsorption isotherm and is physical adsorption.

The values of inhibition efficiencies obtained from the different independent techniques used showed the validity of the obtained results.

REFERENCES

[1] Trabanelli, G., *Corrosion*, **47**, 410, 1991.
[2] Singh, D.N., Dey, A.K., *Corrosion*, **49**, 594, 1993.
[3] Banerjee, G., Malhotra, S.N., *Corrosion*, **48**, 10, 1992.
[4] Arab, S.T., Noor, E.A., *Corrosion*, **49**, 122, 1993.
[5] Raspini, I.A., *Corrosion*, **49**, 821, 1993.
[6] Hajjaji, N. et al, *Corrosion*, **49**, 326, 1993.
[7] Elachouri, M et al, *Corros. Sci.*, **37**, 381, 1995.
[8] Luo, H., Guan, Y.C., Han, K.N., *Corrosion*, **54**, 619, 1998.
[9] Migahed, M.A., Azzam, E.M.S., Al-Sabagh, A.M., *Mater. Chem.Phys.*, **85**, 273, 2004.
[10] Villamil, R.F.V et al, *J. Electroanal. Chem.*, **472**, 112, 1999.
[11] Zhao, T.P., Mu, G.N., *Corros. Sci.*, **41**, 1937, 1999.
[12] Abd El Rehim, S.S., Hassan, H., Amin, M.A., *Mater.Chem.Phys.*, **70**, 64, 2001.
[13] Abd El Rehim, S.S., Hassan, H., Amin, M.A., *Mater.Chem.Phys.*, **78**, 337, 2003.
[14] Guo, R., Liu, T., Wei, X., *Colloids Surf.*, A, **209**, 37, 2002.
[15] Branzoi, V., Golgovici, F., Branzoi, F., *Mater.Chem.Phys.*, **78**, 122, 2002.
[16] Parikh, K.S., Joshi, K.J., *Trans. SAEST*, **39**, 29, 2004.
[17] Ekpe, U.J., Ebenso, E.E., Ibok, U.J., *J. West Afr. Assoc.*, **37**, 13, 1994.
[18] Loto, C.A., *Niger. Cor. J.* **19**, 20, 1998.
[19] Al-Sehaibani, H., *Materialwiss. Werkstofftech.*, **31**, 1060, 2000.
[20] Orubite, K.O., Oforka, N.C., *Mater. Lett.*, **58**, 1768, 2004.
[21] Gunasekaran, G., Chauhan, L.R., *Electrochim. Acta*, **49**, 4387, 2004.
[22] Abdel-Gaber, A.M. et al, *Corrosion*, **62**, 293, 2006.
[23] Bouyanzer, A., Hammouti, B., Majidi, L., *Mater. Lett.*, **60**, 2006 2840,.
[24] El-Etre, A.Y., J. *Colloid Interface Sci.*, **314**, 578, 2007.
[25] Okafor, P.C. et al, *Corros. Sci.*, **50**, 2310, 2008.
[26] Oguzie, E.E., *Corros. Sci.*, **50**, 2993, 2008.

[27] Abdel-Gaber, A.M., Abd-El-Nabey, B.A., Saadawy, M., *Corros. Sci.*, **51**, 1038, 2009.
[28] Eddy, N.O. et al, *J. Appl. Electrochem.*, **39**, 849, 2009.
[29] Raja, P.B., Sethuraman, M.G., *Mater. Corros*., **60**, 22, 2009.
[30] Satapathy, A.K. et al, *Corros. Sci.*, **51**, 2848, 2009.
[31] Lebrini, M., Robert, F., Lecante, A., Roos, C., *Corros. Sci.*, **53**, 687, 2011.
[32] Behpour, M. et al, *Corros. Sci.*, **53,** 2489, 2011.
[33] Torres, V.V. et al, E., *Corros. Sci.*, **53**, 2385, 2011.
[34] Rocha, J.C., Gomes, J.A.C.P., D'Elia, E., *Corros. Sci.*, **52**, 2341, 2010.
[35] Abdel-Gaber, A.M. et al, *Corros. Sci.*, **48**, 2765, 2006.
[36] Dahiya, P., Purkayastha, S., *Asian J Pharm Clin Res*, **5**, 62, 2012.
[37] Mu, G.N., Zhao, T.P., Liu, M., Gu, T., *Corrosion*, **52**, 853, 1996.
[38] Parr, R.G., Donnelly, R.A., Levy, M., Palke, W.E., *J. Chem. Phys*., **68**, 3801, 1978.
[39] Aljourani, J., Raeissi, K., Golozar, M.A., *Corros. Sci.*, **51**, 1836, 2009.
[40] Amar, H. et al, *Corros.Sci*., **49**, 2936, 2007.
[41] Migahed, M.A., Azzam, E.M.S., Morsy, S.M.I., *Corros.Sci*., **51**, 1636, 2009.
[42] Moussa, M.N.H., El-Far, A.A., El-Shafei, A.A., *Mater.Chem.Phys*., **105**, 105, 2007.
[43] Benabdellah, M. et al, *Mater.Chem.Phys*., **105**, 373, 2007.
[44] Bayol, E., Kayakirilmaz, K., Erbil, M., *Mater.Chem.Phys*., **104**, 74, 2007.
[45] Benalli, O. et al, *Appl. Surf. Sci.*, **253**, 6130, 2007.
[46] Hsu, C.S., Mansfeld, F., *Corrosion*, **57**, 747, 2001.
[47] Epelboin, I., Keddam, M., Takenouti, H., *J. Appl. Electrochem*. **2**, 71, 1972.
[48] Bessone, J. C. Mayer, K., Tuttner, W. J. lorenz, *Electrochim. Acta*, **28**, 171, 1983.
[49] Bosch Hubrecht, R.W. J., Bogaerts, W.F., Syrett, B.C., *Corros. Sci*., **57**, 60, 2001.
[50] Dinnappa, R. K., Mayanna, S. M., *J. Appl. Elcreochem*., **11**, 111, 1982.
[51] Patel, N., Rawat, A., Jauhari, S., Mehta, G., *European J. Chem*., **1**, 129, 2010.
[52] Atkins, P.W., *Physical Chemistry*, 6th ed., Oxford University Press, 1999.
[53] Bhat, J. I., Alva, V. D. P., *J. Korean. Chem. Soc*., **55**, 835, 2011.
[54] Oguzie, E. E. et al, *Mater. Chem. Phys.*, **87**, 394, 2004.
[55] Aramaki, K., Hackerman, N., *J. Electrochem. Soc.*, **116**, 568, 1969.
[56] Tang, L., Li, X., Li, L., Mu, G., Liu, G., *Mater. Chem. Phys*., **97**, 301, 2006.
[57] Lipkowski, J., Ross, P.N., *Adsorption of Molecules at Metal Electrodes*, VCH, New York, 1992.
[58] Da Costa, S. L. F. A., Agostinho, S. M. L., *Corros. Sci*., **45**, 472, 1989.
[59] El-Sherbiny, E.F., *Mater. Chem. Phys.,* **60**, 286, 1999.
[60] Fouda, A.S., Al-Sarawy, A.A., El-Katori, E.E., *Desalination*, **201**, 1, 2006.
[61] Anand, R. R., Hurd, R. M., Hackerman, N., *J. Electrochem .Soc*., **112**, 138,1965.
[62] Cook, E. L., Hackerman, N., *J. Phys. Chem*., **55**, 549, 1951.
[63] Bordeaux, J.J., Hackerman, N., *J. Phys. Chem*., **61**, 1323, 1957.
[64] Mu, G.N., Zhao, T.P., Liu, M., Gu, T., *Corrosion*, **52**, 853, 1996.
[65] Singh, A.K., Quraishi, M.A., *Corros. Sci*., **52**, 1529, 2010.